Journal of
Materials Chemistry A

Accepted Manuscript

This article can be cited before page numbers have been issued, to do this please use: W. Gong, Q. Wu, G. Jiang and G. Li, *J. Mater. Chem. A*, 2019, DOI: 10.1039/C9TA02457C.

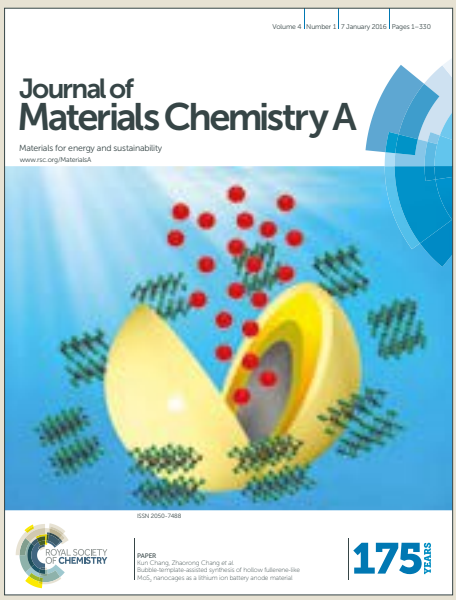

ROYAL SOCIETY OF CHEMISTRY

rsc.li/materials-a

View Article Online
DOI: 10.1039/C9TA02457C

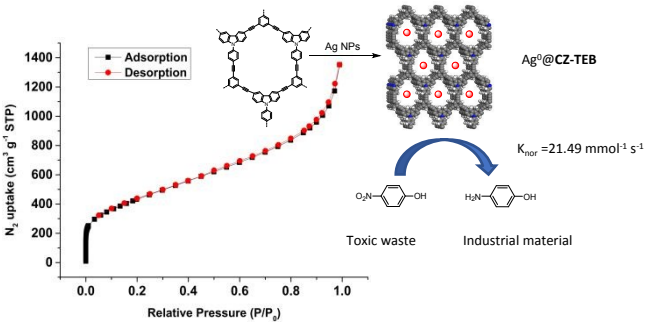

A novel covalent micro/macro porous polymer (CMP), **CZ-TEB**, is synthesized and then Ag NPs are immobilized on it, the normalized rate constant (K_{nor}) of Ag^0@**CZ-TEB** catalyzed reduction reaction of 4-NP to 4-AP reaches up to 21.49 $mmol^{-1}$ s^{-1}.

View Article Online
DOI: 10.1039/C9TA02457C

COMMUNICATION

Ultrafine Silver Nanoparticles Supported on a Covalent Carbazole Framework as High-Efficiency Nanocatalysts for Nitrophenol Reduction

Received 00th January 20xx,
Accepted 00th January 20xx

DOI: 10.1039/x0xx00000x

Wei Gong, Qianqian Wu, Guoxing Jiang and Guangji Li*

A novel conjugated microporous polymer (CMP) material CZ-TEB was synthesized with carbazole analogue and 1,3,5-triethynylbenzene. It possessed high specific surface area, excellent thermo-stability and layered-sheet morphology. Furthermore, ultrafine silver nanoparticles were successfully immobilized on the CZ-TEB, so preparing a nanocatalyst Ag^0@CZ-TEB. To evaluate its catalytic performance, the Ag^0@CZ-TEB was exploited in the reduction reaction of nitrophenols, a family of priority pollutants. The Ag^0@CZ-TEB exhibited high catalytic ability, convenient recovery and excellent reusability. Strikingly, the normalized rate constant (k_{nor}) of the reduction reaction of 4-NP to 4-AP is as high as 21.49 $mmol^{-1}$ s^{-1}. This result shows a significant improvement over all previously reported work. We purposed to use a "capture-release" model to explain the high catalytic ability of the Ag^0@CZ-TEB. This explanation is supported by the further experimental results that agree well with the "capture-release" model.

Introduction

Ultrafine metal nanoparticles (UMNPs) materials are a kind of metal nanoparticles with narrow size distribution. Taking advantages of the high surface-to-volume ratio and high-density active sites, UMNPs are considered as a promising atom-efficient catalyst.[1] However, owing to the high surface energy, UMNPs are thermodynamically unstable and easy to aggregate; the surface of UMNPs is particularly prone to contamination *via* the direct attachment of capping molecules with strong chemical interactions. These defects make UMNPs lose their catalytic activity, recyclability and reusability during catalytic reactions.[2-4] Despite some pioneering work has been made to overcome these shortcomings, it is still a major challenge to design and fabricate highly efficient and easily reusable UMNPs. Recently, porous framework supported UMNPs materials have aroused great interest due to their excellent performance as nanocatalysts in catalytic processes.[5,6] This advanced method can minimize the agglomeration of UMNPs and make the catalytic materials easy to clean and reuse. Such composite nanocatalysts provide exciting possibilities to achieve the application of UMNPs catalyst, and also opportunities for the further investigation of both new and existing reactions.

Constructed by diverse organic building blocks, porous organic polymers (POPs), which are classified as polymers of intrinsic microporosity (PIMs),[7-10] covalent organic framework (COFs),[11-15] conjugated micro- and meso-porous polymers (CMPs),[16-19] are an emerging class of porous materials. Compared with traditional porous materials such as zeolites and porous carbon, POPs are inherently designable owing to the diversity of functional building blocks. It implies that the POPs with various structures can be designed and synthesized to meet the multiple purposes. Moreover, POPs are usually constructed by light element such as nitrogen and carbon, thus exhibiting relative light-weight and atom-efficiency. The studies on POPs materials have been expanded to their functional applications in many fields, including storage, separation, and purification of gas,[20-22] sensing device[23, 24] and photoelectricity.[25-28] As one of the most promising fields, the POPs-supported catalysts have also been continuously studied.[17,29,30] Some researchers found that the catalytic reaction proceeding in confined spaces performed better than traditional catalytic reaction.[31,32] This finding implies that porous materals can be used as efficient supported materials for metal catalyst. Sharing the same advantages, the porous structure and diverse building blocks in CMPs, which have non-negligible effect on the material property, makes it possible to meet different purposes, especially in supported metal heterogeneous catalyst. [33]

In this contribution, a novel conjugated micro-porous polymer (CMP) with rigid 2D chemical structure, **CZ-TEB**, was synthesized using carbazole analogue (CZ) and 1,3,5-triethynylbenzene (TEB) as building blocks. Further analysis indicated that **CZ-TEB** possessed excellent thermo-stability and high Brunauer-Emmett-Teller (BET) surface area. Moreover, Ag^0 nanoparticles were immobilized on the **CZ-TEB**, thus obtaining a new silver catalyst Ag^0@**CZ-TEB**. The catalytic activity and

* *Department of Polymer Science and Engineering, School of Materials Science and Engineering, South China University of Technology, Guangzhou 510640, Guangdong, P. R. China. E-mail: gjli@scut.edu.cn*

† Electronic Supplementary Information (ESI) available: detailed experimental procedures, full characterization data and the other experimental results. See DOI: 10.1039/x0xx00000x

View Article Online
DOI: 10.1039/C9TA02457C

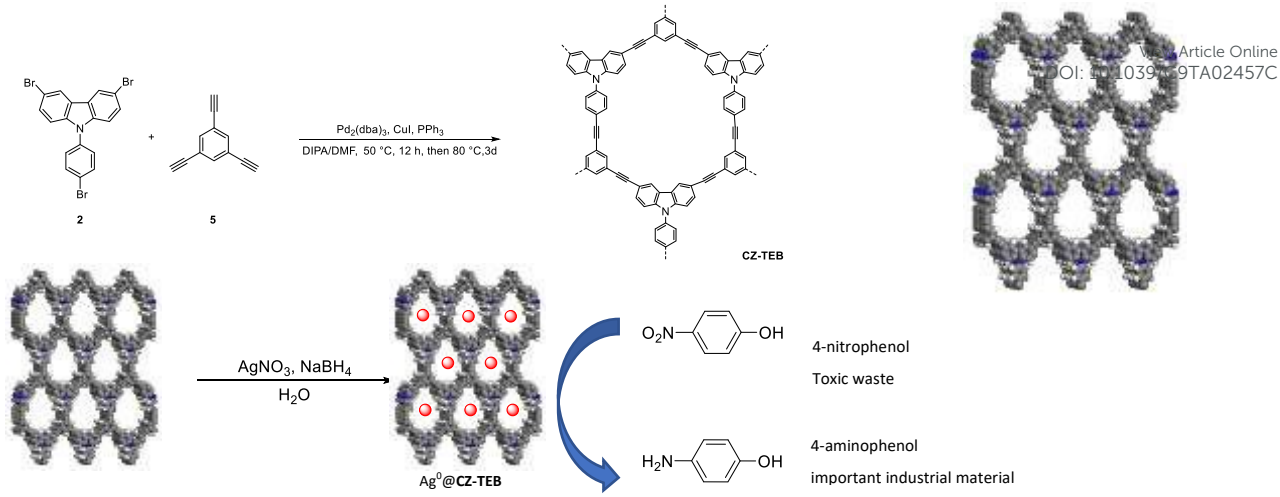

Scheme 1 Illustration of synthetic pathway and pore structure of **CZ-TEB** for silver nanoparticle immobilization. C, grey; N, blue; H, white; silver nanoparticles, red.

reusability of the as-prepared nanocatalyst Ag^0@**CZ-TEB** were studied using the reduction of an environmental pollutant 4-nitrophenol as a model reaction.

Results and discussion

The synthesis of **CZ-TEB** was achieved *via* Sonagashira coupling reaction of carbazole analogue **2** with 1,3,5-triethynylbenzene (**5**), as shown in Scheme 1. The results of the reaction condition screening indicated that among the products, the **CZ-TEB**, which was synthesized in the mixed solvent of DMF/diisopropylamine (DIPA) at 80 °C for 3 days using tris(dibenzylideneacetone) dipalladium(0) ($Pd_2(dba)_3$) as a catalyst, possesses the highest specific surface area, 1600 m^2 g^{-1} (Table S1†, Enrty 5; for more details of condition screening, see ESI). It is noteworthy that the different palladium catalysts have a huge impact on the BET surface area of the **CZ-TEB**, while the solvents do not the case. The as-prepared **CZ-TEB** was further characterized by Fourier transform infrared spectroscopy (FT-IR) (Fig. 1a) and ^{13}C cross-polarization magic-angle spinning nuclear resonance (^{13}C CP/MAS NMR) (Fig. 1e). According to the FT-IR spectrum of the **CZ-TEB**, the nearly completed disappearance of R-C≡C-H resonance at 3275 cm^{-1} indicates that most of the compound **5** has been used up. Correspondingly, the weak stretching vibration bands around 2197 cm^{-1} is observed, implying the existence of R-C≡C-R in the **CZ-TEB**. In the ^{13}C CP/MAS NMR spectrum of the **CZ-TEB** (Fig. 1e), there are three intense peaks between 120 to 150 ppm assigned to the aromatic carbons and two minor peaks at ca. 115 and 93 ppm, indicating the existence of alkynyl groups.

However, in spite of all efforts, the powder X-ray diffraction (PXRD) for the **CZ-TEB** within the 2θ range of 5-60° shows a dispersion peak. It follows that the **CZ-TEB** is amorphous rather than crystalline. The layered-sheet morphology of the **CZ-TEB** was observed by field-emission scanning electron microscopy (FE-SEM) (Fig. 2a). It can be attributed to the π-π stacking between the aromatic ring structure of adjacent layers. Besides, the **CZ-TEB** exhibited robust thermal stability. Only 13.2 *wt*% loss was detected up to 700 °C as revealed by thermal gravimetric analysis (TGA) (Fig. 1d).

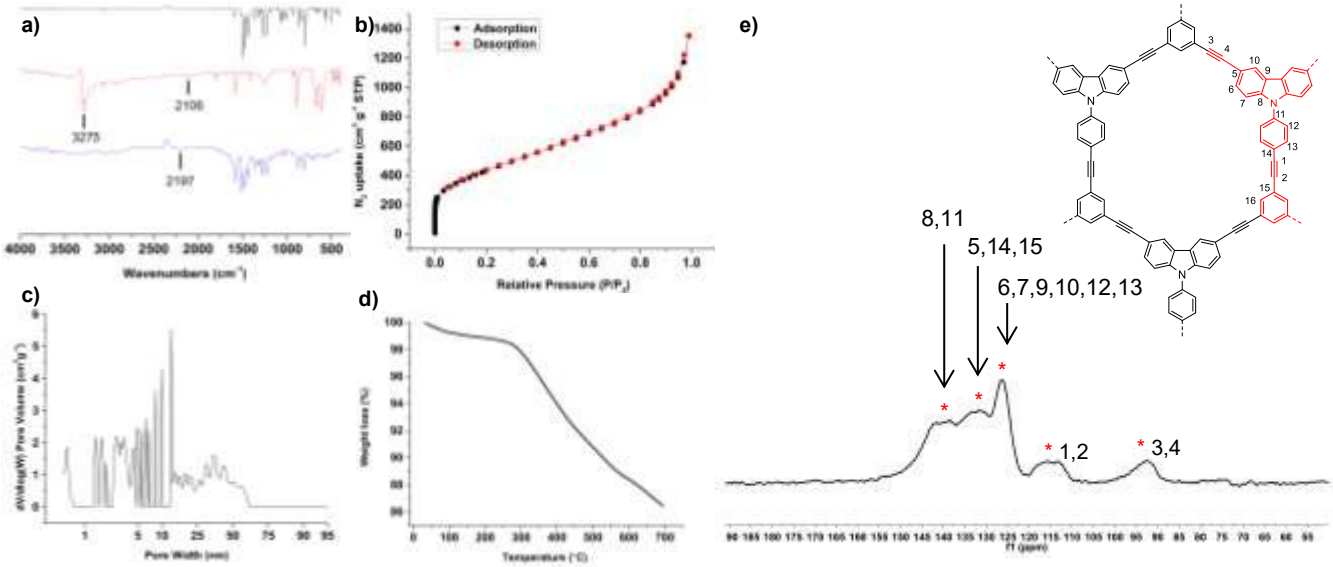

Fig. 1 a) FT-IR spectra of compounds **2** (black), **5** (red), and **CZ-TEB** (blue); b) N_2 adsorption-desorption analysis; c) pore-size-distribution of **CZ-TEB**; d) TGA curve of **CZ-TEB**; e) ^{13}C CP/MAS NMR spectrum of **CZ-TEB**.

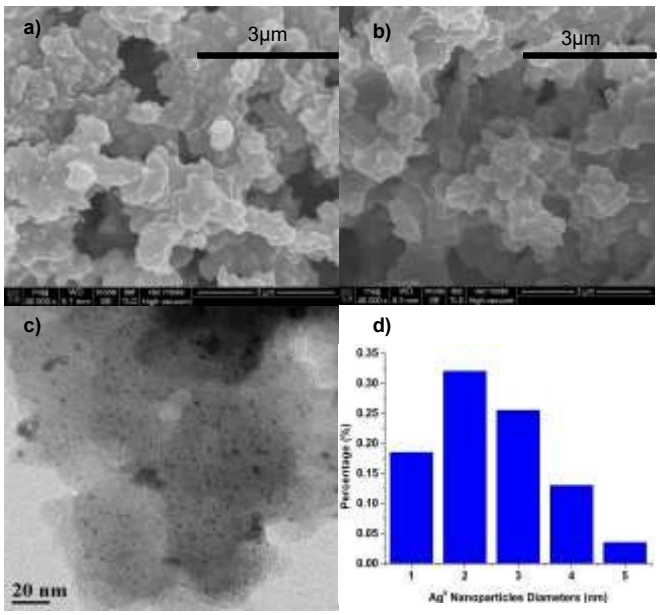

Fig. 2 a) SEM image of the as-prepared **CZ-TEB**; b) SEM image of Ag^0@**CZ-TEB** after five catalytic runs; c) TEM image of Ag^0@**CZ-TEB**; d) Size distribution of silver nanoparticles (statistical data for over 100 particles).

As an important structural feature of POPs, the porosity of the **CZ-TEB** was also investigated. First, the nitrogen sorption experiment at 77 K was conducted. The specific surface areas and pore dimensions were evaluated based on both BET and Langmuir methods, respectively. As shown in Fig. 1b, the nitrogen adsorption-desorption isotherms of the **CZ-TEB** show a typical type IV adsorption at low relative pressure ($P/P_0 < 0.2$) with an steep rised curve, implying that nitrogen molecules occupy the small pores. The adsorption gradually rises over the remaining relative pressure ($0.2 < P/P_0 < 0.85$), another steep rise occurs at relative high pressure ($P/P_0 > 0.85$). This increasing adsorption of nitrogen can be attributed to the inter-layer gap.[34] The pore size distribution of the **CZ-TEB** was calculated by using a nonlocal density functional theory (NL-DFT) method. It can be seen from the result in Fig. 1c that the **CZ-TEB** exhibits a wide pore size distribution, as observed in purely amorphous porous polymers.[35,36] Meanwhile, the specific surface area of the **CZ-TEB** determined by BET method and Langmuir method, respectively, is 1600 $m^2\ g^{-1}$ and 1537 $m^2\ g^{-1}$, respectively (Fig. S15†); and the total pore volume was determined to be 2.09 $cm^3\ g^{-1}$ ($P/P_0 = 0.99$).

Like other POPs materials, the **CZ-TEB** with high specific surface area and nanoscale porous structure may be an appropriate supported material for catalytic metal. Therefore, a new silver catalyst Ag^0@**CZ-TEB** was prepared using the **CZ-TEB** as a supported framework for silver nanoparticles (Scheme 1, for the synthesis details, see ESI). High-resolution TEM image (HR-TEM) confirmed the Ag nanoparticles were in crystalline phase with a crystal plane spacing of 0.236 nm, which corresponds to the [111] lattice plane of Ag^0 NPs (Fig. S9f†). X-ray photoelectron spectroscopy (XPS) analysis also confirmed the presence of Ag^0 nanoparticles in the Ag^0@**CZ-TEB** in which the characteristics of Ag^0 species were observed at binding energies of 368 eV ($3d^{5/2}$) and 374 eV ($3d^{3/2}$), respectively (Fig. S17†). The loading of Ag^0 was determined by Inductively Coupled Plasma-Atomic Emission Spectrometry (ICP-AES) to be 5.1 *wt%*.

Owing to the fact that the **CZ-TEB** can be easily dispersed in low-polar solvent or aprotic solvent, but aggregate in protic solvent such as water. it could be inferred that the ideal model reaction for evaluating the catalytic performance of the prepared nanocatalyst Ag^0@**CZ-TEB** should have the following features: (a) the substrate molecules can enter the pores of the catalyst and interact with the metal or catalytically active sites in the pores; (b) once the reaction is completed, the product can easily detach from the catalyst surface so as to make the catalytically active site available for another substrate molecule. Based on the above inference, the reduction reaction of nitrophenols in water should be a model reaction for evaluating the catalytic performance of Ag^0@**CZ-TEB,** where nitrophenols are hydrophobic and the reduction products or aminophenols are prone to form hydrogen bonds with water, thereby easily detaching from the catalyst surface. Besides, this reaction is one of the widely used reactions for evaluating silver-loaded catalysts. On the other hand, nitrophenols are toxic nitroaromatics and also persistent organic pollutants in industrial wastes. The chemical and biological stability makes them difficult to

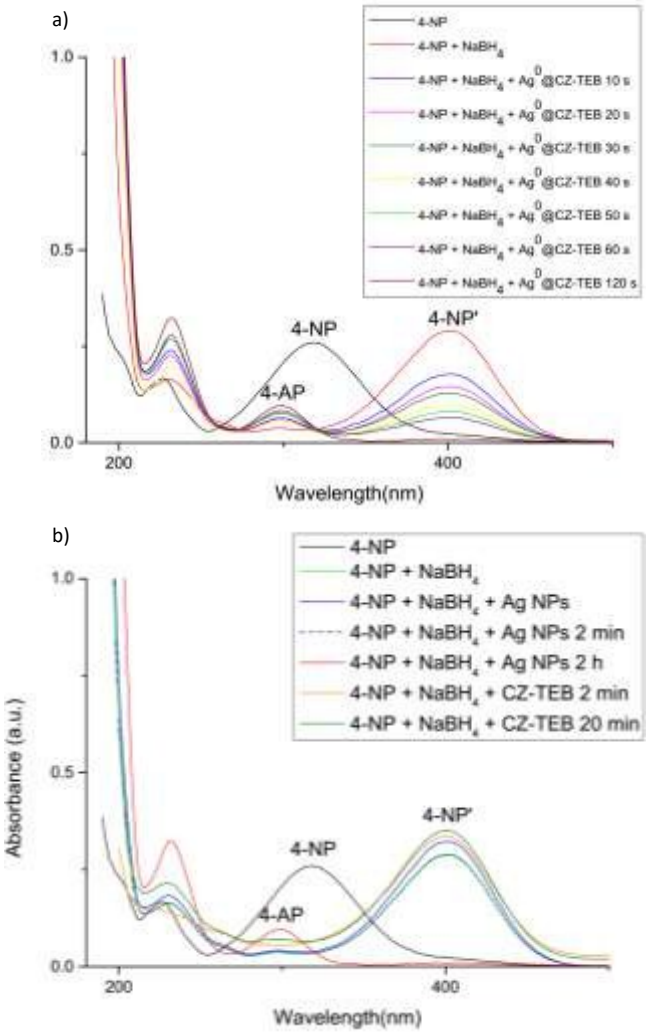

Fig. 3 a) UV-vis specta of Ag^0@**CZ-TEB** catalyzed reduction reaction of 4-NP to 4-AP; b) UV-vis specta of the corresponding reduction reaction as control experiments, where unsupported Ag NPs or **CZ-TEB** was used as catalyst, respectively.

View Article Online
DOI: 10.1039/C9TA02457C

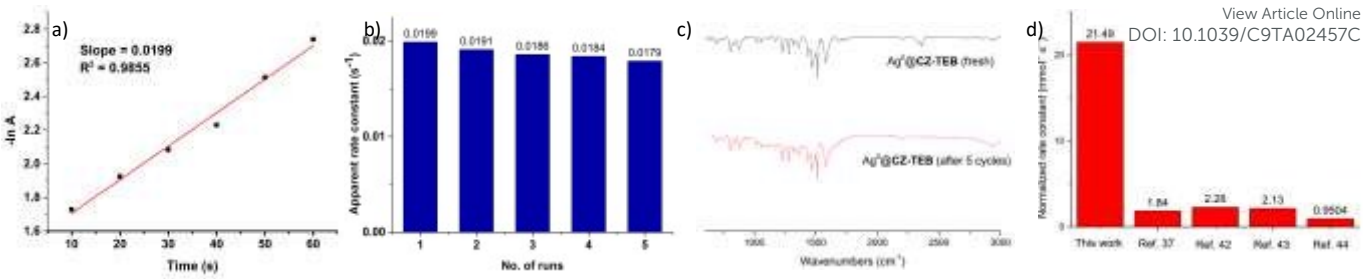

Fig. 4 a) Pseudo-first-order plot of -ln A versus time at ambient temperature and pressure; b) rate constant *k* for the reduction reactions of 4-NP in five consecutive runs; c) FT-IR spectra of fresh Ag^0@**CZ-TEB** and Ag^0@**CZ-TEB** after 5 consecutive runs. d) comparison of normalized rate constant with other studies.

degrade in a natural environment. Many methods such as microbial degradation, extraction, adsorption, catalytic oxidation or reduction have been used in the treatment of nitrophenols. It is noteworthy that the aminophenols produced *via* the reduction reaction of nitrophenols is a class of synthetic intermediates for manufacturing pharmaceuticals, dyes, polymer stabilizers and imaging agents.[37] Hence, the reduction of nitrophenols to aminophenols is considered to be a very promising way to treat nitrophenols. Currently, the reduction reactions of nitrophenols using expensive Au, Pt or Pd as catalysts have been studied extensively; but there is not much research on the relatively cheap Ag catalysts.[38] Therefore, novel silver nanocatalysts with the characteristics of cheapness, high efficiency and reusability are of great significance for the reduction of nitrophenols into aminophenols; and the potential applications in the environmental management and sustainable chemistry also make them attract great interest.

Table 1 Data on the rate constants of the reduction reactions of nitrophenols with different sterically hindered substituent groups using Ag^0@**CZ-TEB** as nanocatalyst.

Entry	Substrate	*T* (°C)[a]	*K* (s^{-1})	k_{nor} ($mmol^{-1}\ s^{-1}$)
1	4-NP	RT	1.99×10^{-2}	21.49
2	2-Me-4-NP	RT	1.88×10^{-2}	20.30
3	2-Cl-4-NP	RT	6.67×10^{-4}	0.36
4	2-Br-4-NP	RT	4.17×10^{-4}	0.23
5	2-NP	RT	4.23×10^{-4}	0.23
6	3-NP	RT	2.46×10^{-4}	0.13

[a]*T* = 25±1°C

The reduction of 4-nitrophenol (4-NP) was performed in the presence of large excess $NaBH_4$ (100 equivs to 4-NP) and the prepared nanocatalyst Ag^0@**CZ-TEB**, with distilled water as solvent. The reaction was monitored by UV-vis spectra. As shown in Fig. 3a, the characteristic absorbance peak at ca. 316 nm of 4-NP switched to ca. 400 nm after the addition of $NaBH_4$, and the corresponding reaction solution turned from yellow to fluorescent yellow. After adding Ag^0@**CZ-TEB**, a new characteristic peak appeared at ca. 295 nm, confirming the generaion of 4-aminophenol (4-AP).[37] As the reaction proceeded, the absorbance intensity at ca. 400 nm decreased gradually, while the peak intensity at ca. 295 nm increased gradually. It indicates a constantly increase of the generated 4-AP. After only 2 min reaction time, the absorbance peak at ca. 400 nm of 4-NP disappeared, implying the the reaction was completed (Fig. 3a). The reactions were considered as pseudo-first order in the presence of large excess $NaBH_4$ and the apparent rate constant value was calculated from the ploting slope of $-\ln A_{400}$ against time to be 0.0199 s^{-1}(Fig. 4a), with a normalized rate constant (k_{nor}) of 21.49 $mmol^{-1}\ s^{-1}$ (Table 1, Entry 1).

In order to clarify the catalysis of Ag^0@**CZ-TEB**, a set of control experiments were carried out under the same conditions. In the control experiments conducted without the nanocatalyst Ag^0@**CZ-TEB**, the absorbance at ca. 400 nm hardly changed with time, showing an extremely slow progress of nitrophenol reduction.[37,39-41] In the case of using the unsupported Ag NPs, the reaction was completed after 2 h (Fig. 3b), exhibiting a much slower reaction rate than in the case of using Ag^0@**CZ-TEB** as a catalyst. To our surprise, a very weak absorbance peak at ca. 295 nm representing 4-AP was observed after the **CZ-TEB** catalyzed reduction reaction of 4-NP was

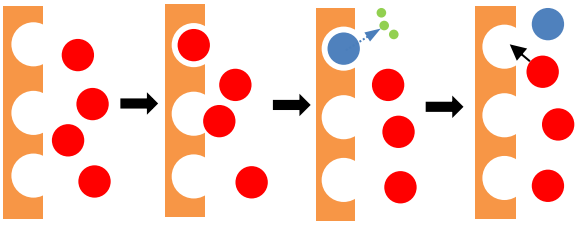

Scheme 2 The schematic diagram of "capture-release" reaction model. brown, porous catalyst; red dot, 4-NP; blue dot, 4-AP, green dot, H_2O; blue arrow, hydrogen bond.

conducted for 20 min (Fig. 3b). It suggests that the supported material **CZ-TEB** could have weak catalytic ability. However, the catalytic ability of **CZ-TEB** ($8.9\times10^{-4}\ mg^{-1}\ s^{-1}$) had negligible impact on that of Ag^0@**CZ-TEB**. Compared with the reported studies on the reduction of 4-NP to 4-AP using silver as a metal catalyst,[42-44] this normalized rate constant indicates a significant increase in the catalytic activity of the prepared nanocatalyst Ag^0@**CZ-TEB** (Fig. 4d). What's more, the Ag^0 loading in the nanocatalyst Ag^0@**CZ-TEB** was calculated to be only 5.1 *wt*%.

Theoretically, The catalytic reaction in Ag^0@**CZ-TEB** nanocatalyst follows the Langmuir–Hinshelwood mechanism, in which BH^{4-} ions will be absorbed on the surface of Ag nanoparticles, and 4-NP will be "captured" by the pores on the **CZ-TEB** surface. The BH^{4-} adsorption on the surface of the nanocatalyst further formate the active hydrogen species, which activates the hydrogenation of the "captured" 4-NP leading to the formation of 4-AP. Comparing with reported work[37] where Ag nanoparticles of the similar size was used as a catalyst, the reduction reaction catalyzed by Ag^0@**CZ-TEB** has better catalytic performence. We attributed the high reaction rate for the reduction of 4-NP to 4-AP to high porosity and surface area of the nonacatalyst.[31,32] It is assumed that this result can be explained by the "capture-release" reaction model as illustrated in Scheme 2. The substrate can be simplfied as a ball and the porous catalyst as a pocket. If the pocket dimension matches with the substrate ball, the

substrate can be "captured" by the pocket. Once the substrate 4-NP is "captured", it will be reducted in a confined space. In this way, the substrate molecules can get higher probability of achieving a "effective collison" with catalyst and $NaBH_4$ according to the reaction collision theory. Since the reduction product 4-AP is more prone to form hydrogen bond with H_2O than 4-NP, the 4-AP molecules, once generated, will immediately move out of the "pocket", and then the "vacated pocket" is available to capture 4-NP molecules again. Such a "capture-release" process will continue until the substrate is used up, thereby keeping the "pocket" of the nonacatalyst from being occupied by the product. One of the key points in this model is the size match of the substrate with the pocket. This speculation is confirmed by the experiments on the catalytic reduction of nitrophenols with different steric hindrance. As shown in Table 1, it is obvious that the reduction reaction of 2-Me-4-NP with a relative small steric hindrance shows slightly lower *k* than that of 4-NP (Table 1, Entry 1-2); the reduction reactions of 2-Cl-4-NP and 2-Br-4-NP with a bulky steric hindrance proceeded much more slowly than that of 4-NP (Table 1, Entry 3-4). Based on an analysis of the molecular size of the different substrates, the difference in the reaction rate given in Table 1 results from the match in size between the substrate and the "pocket" of the nanocatalyst or the pores on the **CZ-TEB**. In this reduction reaction, the substrate 4-NP, calculated as ca. 1.4 nm from the long axis, can match fairly with the "pocket", calculated by theoretically model of single unit in **CZ-TEB** as 1.7 nm from the long axis. That is to say, the reaction rates of the reduction of nitrophenols with different steric hindrance decreases with an increase in the size of substituent group. Therefore, these results well agree with analysis of nitrophenol reduction catalyzed by the Ag^0@**CZ-TEB** *via* the "capture-release" reaction model.

As the Ag^0@**CZ-TEB** had been proved to be an efficient catalyst for the reduction of 4-NP, the reduction of the isomers of 4-NP, 2-NP and 3-NP, were also investigated using the Ag^0@**CZ-TEB** as a catalyst, respectively (Table 1, Entry 5-6). The results show that the reduction reactions of 3-NP and 2-NP are obviously much less efficient than that of 4-NP. It is no surprise that the negative charges on nitroxides in 4-NP are delocalized throughout the benzene rings more easier than 2-NP and 3-NP due to both inductive effect and conjugative effect.[45]

As a high-efficiency nanocatalyst for the nitrophenol reduction, the stability and reusability of Ag^0@**CZ-TEB** are of importance for the practical applications. Therefore, the nanocatalyst Ag^0@**CZ-TEB** was used in five consecutive reactions of 4-NP reduction. The nanocatalyst was recycled by centrifugation and washing with ethanol three times and then used for the next run. After five consecutive runs, there are only 9% decline in the apparent rate constant for Ag^0@**CZ-TEB** catalyzed reduction reaction of 4-NP (Fig. 4b) and 0.1 *wt*% loss of Ag NPs loaded onto the **CZ-TEB**, which was detected by the ICP-AES; and the structure of Ag^0@**CZ-TEB** possesses an excellent stability (Fig. 4c). Besides, there is no significant change in the distribution of Ag NPs as revealed by EDX mapping (Fig. S12, fresh Ag^0@**CZ-TEB**; Fig. S13, Ag^0@**CZ-TEB** after 5 cycles). Therefore, the Ag^0@**CZ-TEB** exhibits excellent stability and reusability.

Conclusions

A novel covalent porous framework **CZ-TEB** with high BET surface area and robust thermo-stability was successfully constructed. On this basis, a new nanocatalyst Ag^0@**CZ-TEB** was prepared by immobilizing ultrafine Ag^0 nanoparticles on the **CZ-TEB**. Furthermore, the Ag^0@**CZ-TEB** is exploited in the reduction of nitrophenols, a family of priority pollutants, at ambient temperature and pressure. The studies indicate that the nanocatalyst Ag^0@**CZ-TEB** is of high efficiency, stability and reusability. Strikingly, the normalized rate constant (k_{nor}) for the reductoin reaction of 4-NP to 4-AP reaches up to 21.49 $mmol^{-1}$ s^{-1}.

Conflicts of interest

There are no conflicts to declare.

Acknowledgements

We would like to thank the researchers in the Shiyanjia Lab (www.shiyanjia.com) for their helping with XPS and BET analysis.

Notes and references

1. Q.-L. Zhu and Q. Xu, *Chem*, **2016**, *1*, 220-245.
2. R. J. White, R. Luque, V. L. Budarin, J. H. Clark and D. J. Macquarrie, *Chem. Soc. Rev.*, **2009**, *38*, 481-494.
3. A. Dhakshinamoorthy and H. Garcia, *Chem. Soc. Rev.*, **2012**, *41*, 5262-5284.
4. S. Navalon, A. Dhakshinamoorthy, M. Alvaro and H. Garcia, *Coordin.Chem. Rev.,* **2016***, 312,* 99-148.
5. G. Li, S. Zhao, Y. Zhang and Z. Tang, *Adv. Mater*., 2018, 1800702
6. J. Artz, *ChemCatChem*, **2018**, *10*, 1753-1771.
7. A. Trewin and A. I. Cooper, *Angew. Chem. Int. Ed.,* **2010***, 49, 1533-1535*.
8. T. Ben, C. Pei, D. Zhang, J. Xu, F. Deng, X. Jing and S. Qiu, *Energ. Environ. Sci*. **2011***, 4,* 3991-3999.
9. K. J. Msayib, D. Book, P. M. Budd, N. Chaukura, K. D. Harris, M. Helliwell, S. Tedds, A. Walton, J. E. Warren, M. Xu and N. B. McKeown, *Angew. Chem. Int. Ed.,* **2009**, *48*, 3273-3277.
10. C. G. Bezzu, M. Carta, A. Tonkins, J. C. Jansen, P. Bernardo, F. Bazzarelli and N. B. McKeown, *Adv. Mater.*, **2012**, *24*, 5930-5933.
11. H. M. El-Kaderi, J. R. Hunt, J. L. Mendoza-Cortés, A. P. Côté, R. E. Taylor, M. O'Keeffe and O. M. Yaghi, *Science*, **2007**, *316*, 268-272.
12. A. P. Côté, A. I. Benin, N. W. Ockwig, M. O'Keeffe, A. J. Matzger and O. M. Yaghi, *Science*, **2005**, *310*, 1166-1170.
13. X. Ding, L. Chen, Y. Honsho, X. Feng, O. Saengsawang, J. Guo, A. Saeki, S. Seki, S. Irle, S. Nagase, V. Parasuk and D. Jiang, *J. Am. Chem. Soc.*, **2011**, *133*, 14510-14513.
14. S. Y. Ding and W. Wang, *Chem. Soc. Rev.*, **2013**, *42*, 548-568.
15. A. F. M. El-Mahdy, C. Young, J. Kim, J. You, Y. Yamauchi, S.-W. Kuo, *ACS Appl. Mater. Interfaces* **2019**, DOI: 10.1021/acsami.8b21867.
16. D. Wu, F. Xu, B. Sun, R. Fu, H. He and K. Matyjaszewski, *Chem. Rev.*, **2012**, *112*, 3959-4015.
17. Y. Zhang and S. N. Riduan, *Chem. Soc. Rev.*, **2012**, *41*, 2083-2094.
18. S.-L. Cai, Y.-B. Zhang, A. B. Pun, B. He, J. Yang, F. M. Toma, I. D. Sharp, O. M. Yaghi, J. Fan, S.-R. Zheng, W.-G. Zhang and Y. Liu, *Chem. Sci.*, **2014**, *5*, 4693-4700.
19. S. Y. Ding, J. Gao, Q. Wang, Y. Zhang, W. G. Song, C. Y. Su and W. Wang, *J. Am. Chem. Soc.*, **2011**, *133*, 19816-19822.

View Article Online
DOI: 10.1039/C9TA02457C

20. A. Li, R. F. Lu, Y. Wang, X. Wang, K. L. Han and W. Q. Deng, *Angew. Chem. Int. Ed.*, **2010**, *49*, 3330-3333.
21. Q. Chen, M. Luo, P. Hammershoj, D. Zhou, Y. Han, B. W. Laursen, C. G. Yan and B. H. Han, *J. Am. Chem. Soc.*, **2012**, *134*, 6084-6087.
22. B. S. Ghanem, N. B. McKeown, P. M. Budd, J. D. Selbie and D. Fritsch, *Adv. Mater.*, **2008**, *20*, 2766-2771.
23. T. Ben, K. Shi, Y. Cui, C. Pei, Y. Zuo, H. Guo, D. Zhang, J. Xu, F. Deng, Z. Tian and S. Qiu, *J. Mater. Chem.*, 2011, **21**, 18208-18214.
24. X. Liu, Y. Xu and D. Jiang, *J. Am. Chem. Soc.*, **2012**, *134*, 8738-8741.
25. J. Weber and A. Thomas, *J. Am. Chem. Soc.*, **2008**, *130*, 6334-6335.
26. L. Chen, Y. Honsho, S. Seki and D. Jiang, *J. Am. Chem. Soc.*, **2010**, *132*, 6742-6748.
27. Y. Xu, L. Chen, Z. Guo, A. Nagai and D. Jiang, *J. Am. Chem. Soc.*, **2011**, *133*, 17622-17625.
28. A. Patra and U. Scherf, *Chemistry*, **2012**, *18*, 10074-10080.
29. P. Kaur, J. T. Hupp and S. T. Nguyen, *ACS Catal.*, **2011**, *1*, 819-835.
30. M. Rose, *ChemCatChem,* **2014**,1166-1182..
31. F. Cárdenas-Lizana, C. Berguerand, I. Yuranov and L. Kiwi-Minsker, *J. Catal.*, **2013**, *301*, 103-111.
32. L. Wang, M. Fang, J. Liu, J. He, J. Li and J. Lei, *ACS Appl. Mater. Interfaces.*, **2015**, *7*, 24082-24093.
33. Y. Xu, S. Jin, H. Xu, A. Nagai and D. Jiang, *Chem. Soc. Rev*. **2013**, *42*, 8012-8031.
34. S. Kandambeth, D. B. Shinde, M. K. Panda, B. Lukose, T. Heine and R. Banerjee, *Angew. Chem. Int. Ed.*, **2013**, *52*, 13052-13056.
35. L. Hao, J. Ning, B. Luo, B. Wang, Y. Zhang, Z. Tang, J. Yang, A. Thomas and L. Zhi, *J. Am. Chem. Soc.*, **2015**, *137*, 219-225.
36. K. Wang, L. Yang, X. wang, L. Guo, G. Cheng, C. Zhang, S. Jin, B. Tan and A. Cooper, *Angew. Chem. Int. Ed.* **2017***, 56, 14149-14153*.
37. H. L. Cao, H. B. Huang, Z. Chen, B. Karadeniz, J. Lu and R. Cao, *ACS Appl. Mater. Interfaces.*, **2017**, *9*, 5231-5236.
38. P. Zhao, X. Feng, D. Huang, G. Yang and D. Astruc, *Coordin. Chem. Rev*., **2015**, *287*, 114-136.
39. Y. Lu, Y. Mei, M. Drechsler and M. Ballauff, *Angew. Chem. Int. Ed.,* **2006**, *45,* 813-816.
40. Y. Mei, G. Sharma, Y. Lu, M. Ballauff, M. Drechsler, T. Irrgang and R. Kempe, *Langmuir*, **2005**, *21*, 12229-12234.
41. K. Esumi, R. Isono and T. Yoshimura, *Langmuir*, **2004**, *20*, 237-243.
42. G. Chang, Y. Luo, W. Lu, X. Qin, A. M. Asiri, A. O. Al-Youbi and X. Sun, *Catal. Sci.Technol.*, **2012**, *2*, 800-806.
43. B. Naik, S. Hazra, V. S. Prasad, N. N. Ghosh, *Catal. Commun*. **2011**, *12*, 1104-1108
44. Z. Wang, S. Zhai, B. Zhai, Z. Xiao, F. Zhang, Q. An, *New J. Chem.* **2014**, *38,* 3999.
45. H. Li, S. Gao, Z. Zheng and R. Cao, *Inorg. Chem.* **2014***, 53, 5692-5697.*